DOI: 10.15480/882.9341

Eighth International Symposium on Marine Propulsors
smp'24, Berlin, Germany, March 2024

Open Water Performance of Two Different Ducted Propellers in Oblique Flow

Negin Donyavizadeh[1], Rickard Bensow[1], Arash Eslamdoost[1]

[1]Department of Mechanics and Maritime Sciences, Chalmers University of Technology, Sweden

ABSTRACT

Ducted marine propellers provide increased efficiency, enhanced maneuverability, improved thrust, and reduced cavitation and noise in certain operating conditions. Ducted propellers may also offer advantages over propellers without a duct in waves. The duct surrounding the propeller can help minimize the effects of wave impact and reduce the blade loading variation as well as the risk of cavitation. This can result in improved propulsion efficiency and reduced vibration and noise levels. Additionally, the enhanced thrust generated by ducted propellers can provide better maneuverability and control in rough seas. However, there is limited documented evidence for the evaluation of the performance of ducted propellers in waves. To this end, this paper's objective is to investigate the effect of ducts on the performance of marine propulsors in waves relative to calm water. Besides a conventional duct design, a special duct geometry that consists of a wavy leading edge is also studied. These investigations are carried out in open water through Computational Fluid Dynamics (CFD). A Kaplan series propeller, KA4–55, and the benchmark 19A-duct are used. The effect of waves on propeller performance is simplified by running the simulations in oblique flow conditions. It has been obtained that in oblique flow, with 19A duct, the propulsive performance increased with increasing angle of flow. Results have demonstrated that incorporating LET ducts can enhance duct thrust performance in straight flow conditions, even without any inclination.

Keywords

Ducted Propeller, Wavy Leading Edge, Waves, Oblique Flow, CFD.

1 INTRODUCTION

Ducted marine propellers are a critical component of modern ship propulsion systems, offering a range of advantages such as increased efficiency, enhanced maneuverability, improved thrust, and reduced cavitation and noise in specific operating conditions. These advantages are particularly pronounced in calm water conditions. However, one area that has received limited attention in the literature is the performance of ducted propellers in waves and oblique flow conditions. This paper aims to address this gap by investigating the open-water performance of two different ducted propellers, specifically a conventional duct design and a unique duct geometry with a wavy leading edge, in oblique flow conditions while accounting for the presence of waves.

The interaction between ducted propellers and waves is a complex phenomenon that can significantly impact their performance. In waves, vessels experience dynamic changes in their operating conditions, including variations in inflow velocity and direction, which can affect propulsive efficiency, thrust, and maneuverability. Ducted propellers have the potential to mitigate some of these effects due to their duct design, which can help minimize wave impact and reduce blade loading variations. This results in improved propulsion efficiency and reduced levels of vibration and noise.

Furthermore, the enhanced thrust generated by ducted propellers can provide better maneuverability and control in rough seas. However, despite the theoretical advantages of ducted propellers in wave conditions, there is a noticeable lack of documented evidence to support these claims. This lack of comprehensive studies hinders the understanding of how ducted propellers perform in the presence of waves and oblique flow, which is vital for optimizing their design and application in practical marine engineering.

Several studies have focused on ducted propellers' hydrodynamic performance in various conditions.

To date, several studies have focused on the hydrodynamic performance of ducted propellers in various conditions, including calm water environments. For example, Falchi et al (2022) conducted an experimental investigation into the effect of Leading-Edge Tubercles (LET) on the performance of marine propellers in fully submerged conditions. Stark, Shi, and Atlar (2021) performed a numerical investigation to assess the impact of bioinspired LET on the hydrodynamic performance of a standard ducted propeller. Troll, Shi, & Stark (2022) explored the influence of LET on the wake flow dynamics of a marine rudder.

The research by Stark, Shi, & Troll (2021) examined the cavitation funnel effect caused by the application of

Leading-Edge Tubercles (LET) on ducted marine propeller blades, providing valuable insights. In a related study, Shi et al (2016) observed cavitation and conducted noise measurements on horizontal axis tidal turbines equipped with biomimetic blade leading edges, which is pertinent to the research on LET. Additionally, Stark & Shi (2021) conducted a comprehensive investigation into the hydroacoustic and hydrodynamic effects of LET on marine-ducted thrusters.

Furthermore, studies such as those conducted by Ghassemi, et al (2016) and Martio, et al (2017) have examined the hydrodynamic characteristics of ducted propellers under oblique flow conditions, shedding light on the challenges associated with these conditions. Zhang et al (2020) provided insights into ducted propeller performance in oblique flow conditions.

Other research by Wang et al (2023) focused on the effects of a nozzle on propeller wake in oblique flow conditions, contributing to our understandingof flow dynamics. Gong et al (2020) investigated the hydrodynamic loads and wake dynamics of ducted propellers in oblique flow conditions.

The studies by Dubbioso, et al (2014) and Yao (2015) provided valuable computational insights into the hydrodynamic performance of marine propellers in oblique flow, further expanding our knowledge in this area. Additionally, Kroll & Mahesh (2022) used Large Eddy Simulation to study ducted propellers in crashback conditions, and Jang & Mahesh (2013) investigated ducted propulsors in crashback using LES. Moreover, the paper by Ghassemi et al (2016) calculated the hydrodynamic characteristics of ducted propellers in oblique flow, providing valuable data.

While the literature provides valuable insights into the performance of ducted propellers in various conditions, including waves and oblique flow, there is a noticeable absence of comprehensive studies systematically investigating the open-water performance of ducted propellers under these conditions. Existing research has primarily focused on specific aspects, such as duct design, tubercles, and cavitation performance. However, a holistic evaluation of ducted propellers in wave conditions, as compared to calm water, is necessary to gain a comprehensive understanding of their behavior and potential advantages in realistic operating conditions.

In summary, ducted marine propellers have demonstrated significant advantages in calm water conditions, including enhanced efficiency, thrust, and reduced cavitation and noise. However, their performance in the presence of waves and oblique flow (flow at an angle) remains an underexplored area. This paper aims to fill this gap by conducting a comprehensive investigation into the open-water performance of two different ducted propellers in oblique flow conditions, shedding light on their behavior in the presence of waves. To achieve these objectives, Computational Fluid Dynamics (CFD) simulations are employed in an open-water environment, simplifying the effect of waves through oblique flow conditions. The study utilizes a Kaplan series propeller, KA4–55, in conjunction with a well-established benchmark duct, the 19A-duct, to conduct comprehensive analyses of their hydrodynamic characteristics in the presence of waves.

The findings of this study will contribute to a better understanding of ducted propeller performance and inform future marine engineering practices in wave-prone environments.

2 NUMERICAL APPROACH

In this research, the impact of ducted propellers on marine propulsion performance in oblique flow conditions is investigated. To achieve this objective, the Commercial Computational Fluid Dynamics (CFD) software, STAR-CCM+, as the numerical tool, has been employed.

The research employs the Shear Stress Transport (*SST k-ω*) turbulent model and the unsteady Rigid Body Motion (RBM) method to solve Large Eddy Simulation (LES) equations.

The Rigid Body Motion (RBM) method entails conducting transient analyses to simulate the movement of a rotating propeller, wherein the propeller is displaced by a fixed distance during each discrete time step. This approach is commonly referred to as the sliding mesh technique. In the current study, the rotational rate of the propeller (n) remained constant at 15 revolutions per second (rps), while the advance velocity was systematically modified to elucidate its influence on the prediction of open-water curve characteristics. The Reynolds number, denoted as Re, was estimated to be approximately $5 \times 10^{+5}$ based on the rotational rate.

In the quest to accurately predict unsteady propeller flow dynamics, this study leverages the Rigid Body Motion (RBM) approach, renowned for its precision. To achieve this, a meticulous time-step of 0.5 degrees of rotation per time-step, equivalent to an infinitesimal duration of approximately 9e-5 seconds, is selected. The simulations maintain a y plus (y^+) that is commonly used in boundary layer theory to define the nearest wall layer thickness, on the propeller and duct surface below 1, with a low wall y^+ treatment that relies on the assumption that the boundary layer near the propeller is adequately resolved by the near-wall mesh temporal discretization benefits from a second-order scheme. Additionally, the downstream development of the propeller wake flow is scrutinized, contributing to the comprehensive understanding of unsteady propeller behavior.

As an essential preliminary stage, a ducted propeller system has been designated as the foundation for a validation study. This study involves comparing numerical findings with existing experimental data.

2.1 Geometry and Computational Domain

The ducted propeller with KA4-55 propeller inside the Wageningen 19A duct (Accelerating Duct) is employed in verifying the numerical simulation. The experimental results available for a ducted propeller are presented by Stark & Shi (2021). The characteristics of the propeller are

that the diameter of the propeller is D=0.25 meters with a fixed pitch ratio of P/D=1 and a uniform tip gap between the surface of the inner channel and the tip of the blade.

The 3D geometry of the duct and propeller can be found in Figure 1 and the specifications of the propulsion system in Table 1. Also, the desired propeller has been placed at 0.5 duct chord lengths from the leading edge of the duct.

Figure 1: Geometry of propeller KA4-55 and duct of 19A (Carlton 2018).

Table 1: Geometric Specifications for Propeller ka4.55 with Duct 19A

Propeller KA4-55			
Type of Section	Kaplan	Expanded Area (EAR)	0.55
Blade Number (N)	4	Pitch Ratio(P/D)	1
Diameter (D)	0.25 m	Tip Clearance (t)	2 mm
Duct 19A			
Type of Duct	19A	Duct Chord (L_D)	0.125 m
Outer Diameter (D_O)	0.306 m	Inner Diameter (D_i)	0.254 m

The computational domain takes the shape of a 3D cylinder, with dimensions of 3.5D extending ahead of and 10.5D behind the ducted propeller's position. The radius of the computational domain is considered 4D.

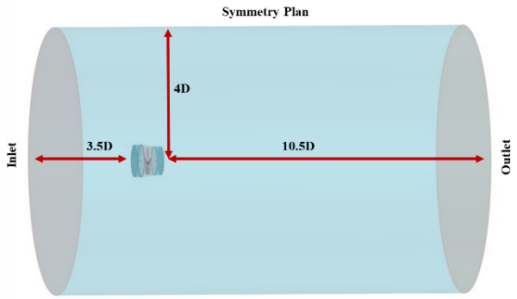

(a)

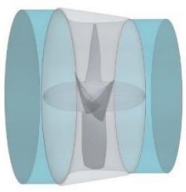

(b)

Figure 2: Computational Domain: a) Fixed Domain, b) RotatingDomain.

This grid was divided into two main sections: The LES simulation utilizes a grid comprising 54 million individual cells, partitioned into two components: a rotating cylindrical region around the propeller and the inner surface of the duct, which consisted of 23 million cells, and the fixed region of the domain including the outer surface of the duct, comprising 31 million cells. The computational domains are shown in Figure 2.

The inlet was defined as a velocity inlet, outlet as pressure outlet, and symmetry plane on the circumferential face as shown in Figure 2. The rotating domain of the propeller and the static region of the surrounding volume were separated by an internal interface. The duct and propeller were defined as non-slip walls.

2.2 Mesh Generation

An unstructured tetrahedral mesh was employed for mesh generation, encompassing around 31 million cells for the fixed domain and a hexagonal mesh was applied on the rotating domain. Prism layers were strategically utilized to address and resolve the boundary layer.

The height of the first boundary layer on the wall is computed based on $y^+ = 1$ assumption and the number of the layers inside the boundary layer flow is considered 12.

Based on the maximum Reynolds number, the first layer height ofthe grid is set as 2.895×10^{-6} m near the blade wall and the duct surface. The blade and duct surface mesh and alsoa section of volume mesh can be shown in Figure 3.

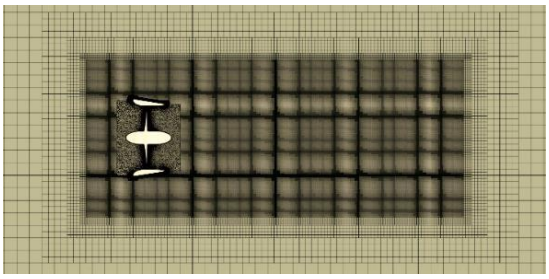

(a)

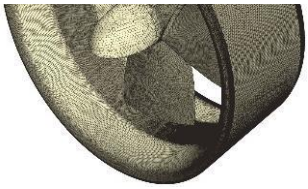

(b)

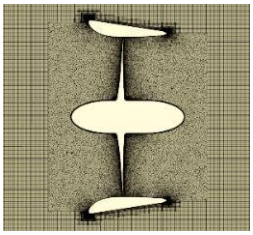

(c)

Figure 3: Mesh grid used in a numerical solution related to propeller KA4.5 and duct 19A.

3 VERIFICATION AND VALIDATION

3.1 Hydrodynamic Coefficients

For computing and defining the thrust and torque of ducted propeller, nondimensional coefficients are used such as advance coefficient (J), thrust coefficient (K_T), torque coefficient (K_Q), and efficiency (η_O) which can be seen in Equation (1) to (6):

$$J = \frac{V_\infty}{n.D} \quad (1)$$

$$K_{T_{Propeller}} = \frac{T_{Propeller}}{\rho.n^2.D^4} \quad (2)$$

$$K_{T_{Duct}} = \frac{T_{Duct}}{\rho.n^2.D^4} \quad (3)$$

$$K_Q = \frac{Q}{\rho.n^2.D^5} \quad (4)$$

$$K_{T_{Total}} = K_{T_{Propeller}} + K_{T_{Duct}} \quad (5)$$

$$\eta_o = \frac{J}{2\pi}\frac{K_{T_{Total}}}{K_{Q_{Total}}} \quad (6)$$

Here, V_A is the advance velocity of the water into the propeller. Equation (6) is used to calculate the propeller efficiency in open water conditions where ρ is the fluid density around the propeller, n is the rotational speed of the propeller, and D is the diameter of the propeller.

3.2 Mesh Study

A validation analysis was conducted to assess the accuracy of the computational simulations. This involved applying the Grid Convergence Index (GCI) method, initially introduced by Roache in 1998 and rooted in Richardson's work from 1911. Additionally, it is recommended in the ITTC procedure outlined (ITTC 1999). The comprehensive methodology adopted for this investigation was originally outlined by Celik and colleagues in 2008 and is detailed in their publication. The primary focus of this analysis was on the total thrust and torque coefficients (referred to as K_{TT} and $10K_Q$) as integral variables. These parameters were examined at an advance ratio of J=0.55, which corresponds to the operational condition associated with maximum efficiency.

To investigate the sensitivity of mesh elements, the uncertainty of numerical simulation U_{SN} is investigated in three parts: Iteration U_I, Grid U_G, and Time Stack U_{TS} uncertainties.

$$U_{SN}^2 = U_I^2 + U_G^2 + U_{TS}^2 \quad (7)$$

The most important part of numerical simulation uncertainty is related to grid uncertainty. In this study, the convergence coefficient, $R_K = \varepsilon_{21_K}/\varepsilon_{32_K}$ is in the range of $0 < R_K < 1$, so it satisfies the monotonic convergence. In Equations (8) to (10), the average value of apparent orders is calculated.

$$P_{avg} = \frac{1}{\ln(r_{21})}\left|ln|\varepsilon_{32}/\varepsilon_{21}| + q(P_{avg})\right| \quad (8)$$

$$q(P_{avg}) = ln\left(\frac{r_{21}^{P_{avg}} - s}{r_{32}^{P_{avg}} - s}\right) \quad (9)$$

$$s = 1.sgn(\frac{\varepsilon_{32}}{\varepsilon_{21}}) \quad (10)$$

For solving Equations (8) and (9), Parameter refinement ratios have defined $r_{21} = \sqrt{2}$ and $r_{32} = \sqrt{2}$.

However, for calculating hydrodynamic parameters such as thrust and torque coefficients, which are denoted by φ, there are two relations of $\varepsilon_{21}=\varphi_2-\varphi_1$ and $\varepsilon_{32}=\varphi_3-\varphi_2$, which are given in Equation (10). The extrapolated hydrodynamic value, the defined approximated relative error, the extrapolated relative error, and the fine-grid convergence index are defined in Equations (11) to (14), respectively.

$$\varphi_{ext}^{21} = \left(r_{21}^{P_{avg}}\varphi_1 - \varphi_2\right) / \left(r_{21}^{P_{avg}} - 1\right) \quad (11)$$

$$e_a^{21} = \left|\frac{\varphi_1 - \varphi_2}{\varphi_1}\right| \quad (12)$$

$$e_{ext}^{21} = \left|\frac{\varphi_{ext}^{21} - \varphi_1}{\varphi_{ext}^{21}}\right| \quad (13)$$

$$GCI_{fine}^{21} = \frac{1.25e_a^{21}}{r_{21}^{P_{avg}} - 1} \quad (14)$$

These parameters are presented for intended hydrodynamics thrust and torque coefficients, in Table 2.

Table 2: GCI method for hydrodynamics thrust and torque coefficients in J=0.55.

Parameter	K_{TT}	$10K_Q$
$\varphi 1$	0.179	0.269
$\varphi 2$	0.167	0.257
$\varphi 3$	0.147	0.230
P_{avg}	1.564	2.428
φ_{ext}^{21}	0.195	0.257
e_a^{21}	0.065	0.043
e_{ext}^{21}	0.083	0.045
GCI_{fine}^{21}	0.113	0.041

The thrust and torque coefficients for the ducted propeller system at J=0.55 for different numbers of elements (coarse, medium, and fine mesh) are presented in Figure 4.

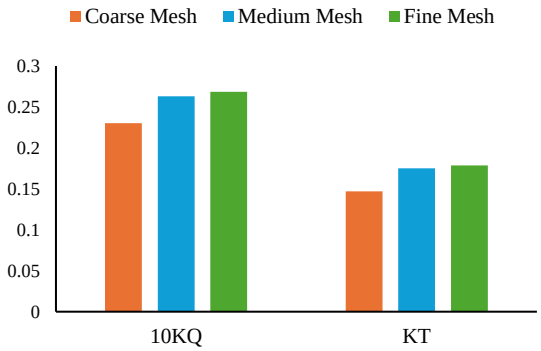

Figure 4: Mesh sensitivity analysis of the ducted propulsion system with propeller KA4.55 and 19A duct.

3.3 Validation

To check the accuracy of the numerical solution, the computed open water curves are compared to experimental data (Stark et al 2021). In Figure 5, the acquired numerical data is displayed and compared to experimental data. The agreement between the computed K_Q and the measured one is better for the comparison error of K_{TT}, where the computed values underpredict the measured data. Consequently, the computed efficiency is higher than the measured one.

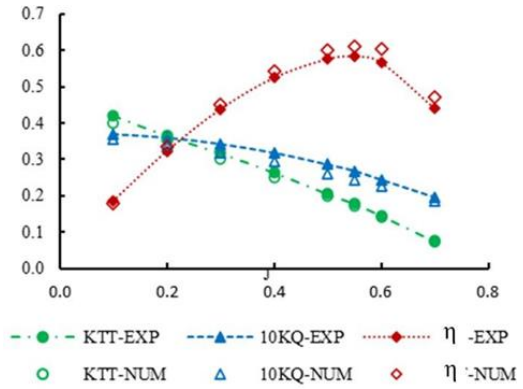

Figure 5: Comparison of the numerical results of K_{TT}, $10K_Q$, and η_o for propeller KA4.55 and 19A duct with experimental results.

Based on the results obtained from the comparison of the LES numerical method and experimental method, it can be seen that the error obtained is around 5% and in the advance ratio between 0.5 and 0.7, the errors are around 10%.

Also, for a more detailed investigation, the results of the experimental solution have been compared with the numerical solution using the RANS method, and in this method, the errors have been found to be around 3%, which is an acceptable amount in numerical solutions.

4 RESULTS AND DISCUSSION

This section explores the impact of the flow angle (φ) upon the hydrodynamic coefficients within the domain. In this study instead of applying the wave condition directly to the propulsion system, the propulsion system is placed in the oblique flow. Due to this angled inlet flow to the propeller and duct conditions similar to wave are simulated. For applying the oblique flow conditions, three different angles (0, 5, 10 degrees) are considered which is shown in Figure 6. Instead of changing the angle of the ducted propeller within the computational domain, the velocity inlet is adjusted to the desired angles.

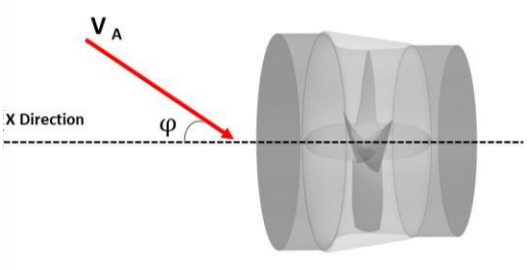

Figure 6: Direction of inlet flow with angle of φ.

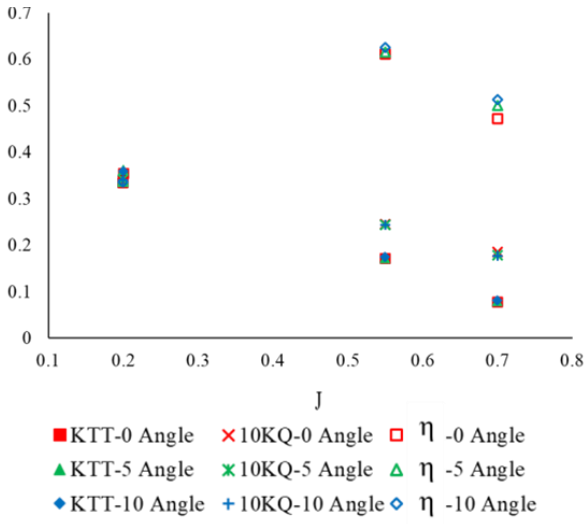

Figure 7: Hydrodynamics coefficients in different angles of flow.

As depicted in Figure 8, there is no significant change in the hydrodynamic coefficients at an advance coefficient of 0.2. However, at advance coefficients of 0.55 and 0.7, a rather significant increment is observed in efficiency which is mainly a consequence of torque reduction as the flow incidence angle increases.

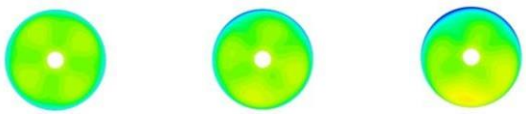

J=0.55
Angle= 0 degree
V_{Axial}= 2.788 m/s

J=0.55
Angle= 5 degree
V_{Axial}= 2.792 m/s

J=0.55
Angle= 10 degree
V_{Axial}= 2.793 m/s

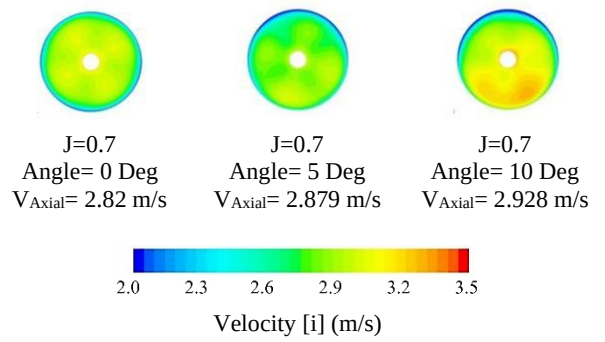

Figure 8: Flow field velocity with varying Angle of inlet flow at J=0.55 and J=0.7.

The axial velocity distribution at the distance of 0.06LDuct from the leading edge of the 19A duct for different angles is shown in Figure 8. As can be seen in this figure, as the flow angle increases, the velocity in the lower part of the disk increases and decreases in the upper part of the disk. For better clarity and understanding, separate thrust bar charts for the propeller and duct and torque coefficients are presented in Figures 9, 10, and 11.

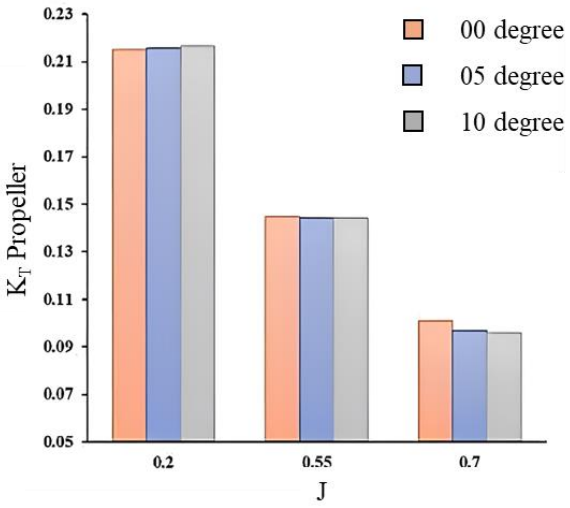

Figure 9: K_T of propeller KA4.55 within oblique flow.

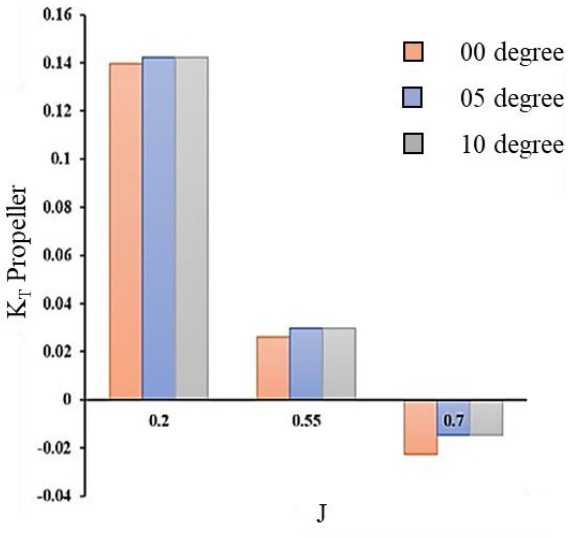

Figure 10: K_T of 19A Duct within Oblique Flow.

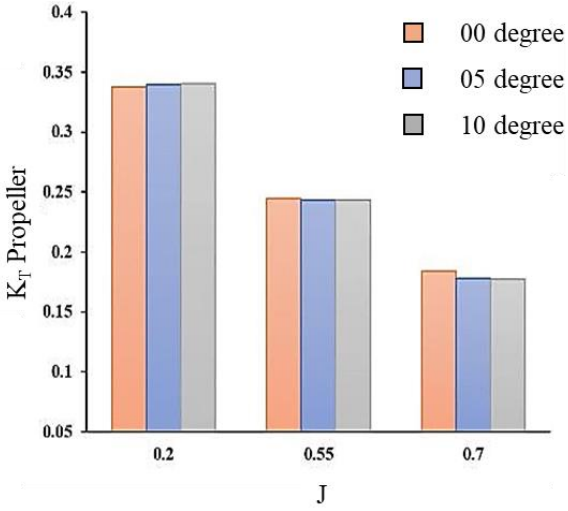

Figure 11: $10K_Q$ of 19A Duct within Oblique Flow

As can be seen in Figures 9 and 10, in an advance ratio less than 0.55, with increasing flow angle, propeller thrust and torque increase. But in advance ratio greater than 0.55, with the increase of flow angle, propeller thrust, and torque decrease. As can be evidenced from Figure 10, in J=0.7, the duct does not generate any thrust and instead generates drag (negative thrust). As can be seen in Figure 11, at an angle of 10 degrees, the efficiency of the system is higher than at other angles. Also, at the advance coefficient of 0.7, it can be seen that the thrust of the duct is negative, so to check the physics of the problem, at an angle of 10 degrees, the pressure distribution at different speeds is presented in Figure 12.

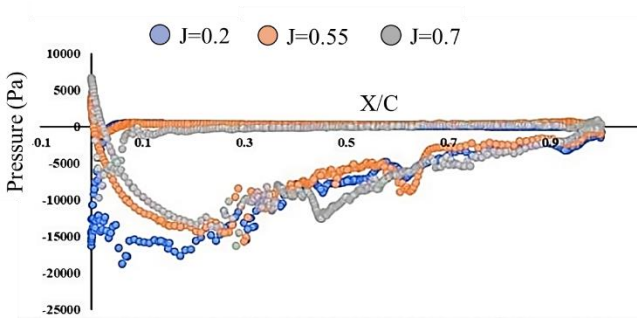

Figure 12: Pressure coefficient of Duct 19A at $\varphi = 10$ deg anddifferent Advance Ratio.

In Figure 12, the pressure distributions around the duct sections are shown. Based on the pressure distributionon the duct profile, with the increase in speed, it can be seen that the pressure decreases near the leading edge of the duct and increases near the trailing edge, and thereforethe thrust result decreases.

Based on the results presented in Figures 9 and 10, it is evident that the angle of flow has a significant impact on the thrust of the propeller and duct, as well as the performance at J=0.55 and 0.7.

Apart from a conventional duct design, we have investigated the performance of a duct with a wavy leading edge at various flow incidence angles at J=0.55 and 0.7, where the flow incidence angle had the more significant effect on the propulsor performance.

Through the optimization study by Stark and Shi (2021), the Tubercle-LE with a wavy length of 0.75LDUCT and Amplitude of 0.04LDUCT has favorable performance in both operating conditions considered when compared to the alternative designs.

This duct geometry has been investigated by Stark & Shi (2021) and is also shown in Figure 13.

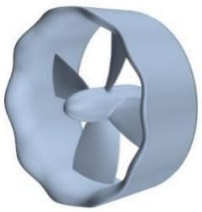

Figure 13: Geometry of Tubercle Duct and Propeller KA4-55.

In Figures 14 to 17, a comparison has been made between the hydrodynamic coefficients of the 19A duct and the LET ductat the advance coefficient of 0.7.

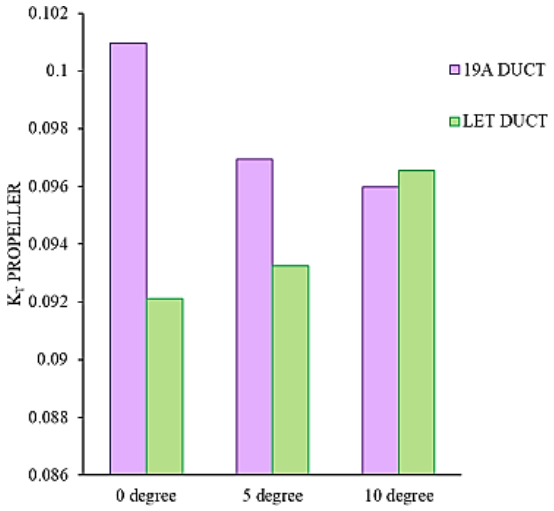

Figure 14: Comparison of K_T of propeller KA4.55 within 19A Duct and LET duct at J=0.7.

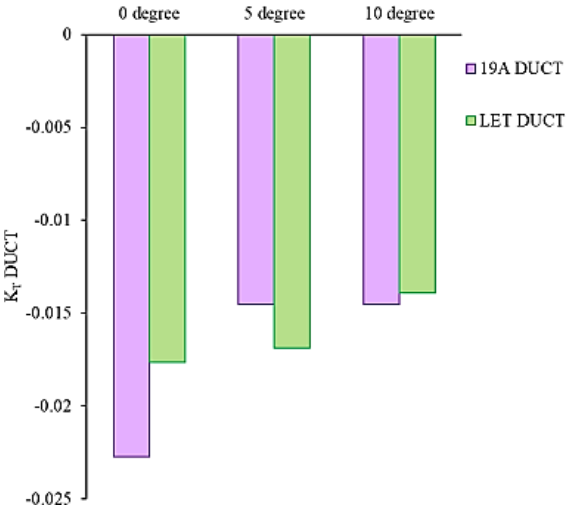

Figure 15: Comparison of K_T of 19A Duct and LET Duct at J=0.7.

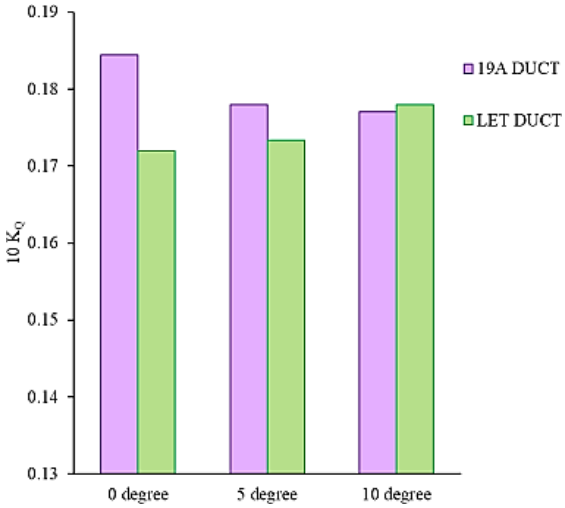

Figure 16: Comparison of 10 K_Q of propeller KA4.55 within 19A Duct and LET duct at J=0.7.

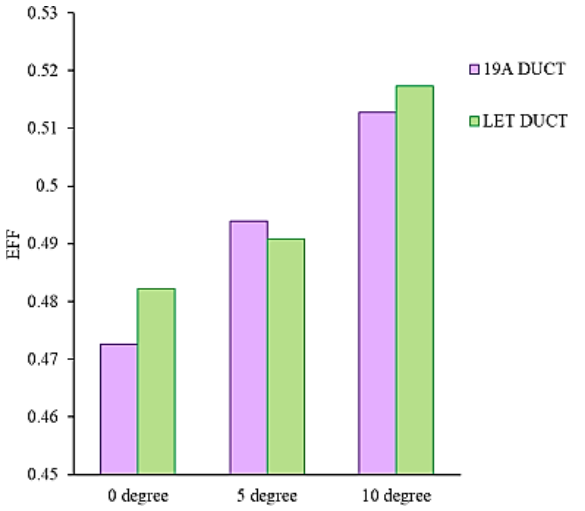

Figure 17: Comparison of η_o of propeller KA4.55 within 19A Duct and LET Duct at J=0.7.

As can be seen in Figure 14, in the simple duct, with the increase of the flow angle, the thrust of the propeller decreases. While, in the wavy leading-edge duct, the thrust of the propeller increases with the increase of this angle.

Also, in φ = 10 degrees, the performance of KA4.55 with the LET duct is 0.78 percent higher than the 19A duct. In Figure 18, the velocity field in the disk of the LET duct is shown at different angles of flow.

Based on Figure 18, At the peak of a wave of leading-edge, there is low velocity that shows the thin boundary layer. But at the angle of 10 degrees, the differences between the velocity of the upper and lower sides of the LET duct at J=0.55 are more than J=0.7.

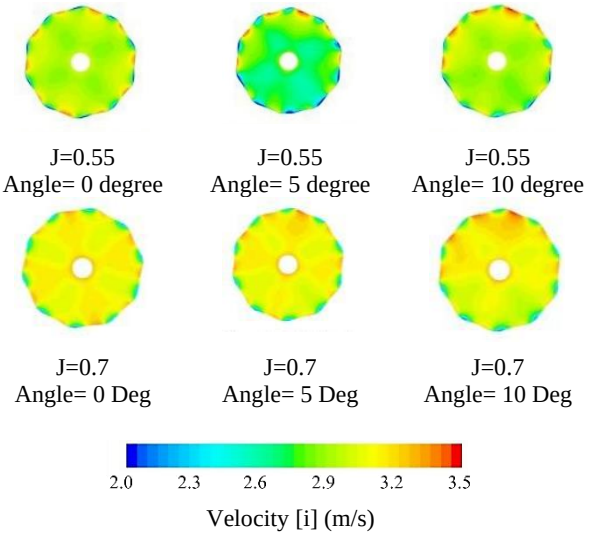

Figure 18: Flow field velocity with varying Angles of inlet flow at J=0.55 and J=0.7 for the tubercle duct.

In Figure 19, the pressure distribution around the Peak of the LET duct is shown for two different advance ratios at φ =10 deg.

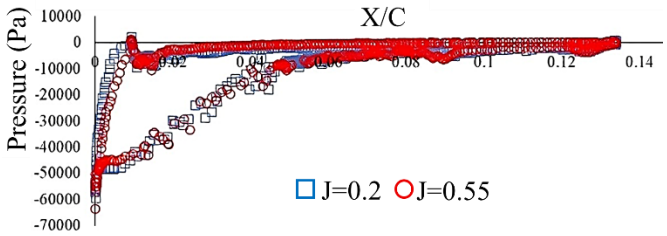

Figure 19: Pressure distribution of peak of LET duct at φ = 10 deg and two different Advance Ratios.

5 CONCLUSIONS

Ducted propellers have demonstrated significant advantages in calm water conditions, including enhanced efficiency, thrust, and reduced cavitation and noise. However, their performance in the presence of waves and oblique flow remains an underexplored area. In the current study, open water performance and hydrodynamics of two different ducted propellers in oblique flow conditions, and their behavior in the presence of waves are investigated.

To achieve these objectives, Computational Fluid Dynamics (CFD) simulations are employed in an open-water environment, simplifying the effect of waves through oblique flow conditions. The study utilizes a Kaplan series propeller, KA4–55, in conjunction with the benchmark 19A-duct, to conduct comprehensive analyses of their hydrodynamic characteristics in the presence of waves.

It has been obtained that in oblique flow, with 19A duct, the propulsive performance increased with increasing angle of flow.

It has shown that the inclusion of LET duct can improve the duct thrust performance at straight flow without any inclination. Also, at the angle of 10 deg, an increase in duct thrustis obtained. Also, in every angle of flow, the thrust of the propeller within the LET duct was increased. The impact on the blade performance is likely due to the interaction between the blades.

The utilization of the LET duct led to an enhancement in propulsion performance, reaching a maximum improvement of 1.9% at a flow angle of 0 degrees and 0.78% at a flow angle of 10 degrees.

REFERENCES

Carlton, J. (2018). Marine Propellers and Propulsion. Butterworth- Heinemann.

Dubbioso, G., Muscari, R. & Mascio, A. D. (2014). 'Analysis of a marine propeller operating in oblique flow Part 2: Very high incidence angles', Computers & Fluids, 92, March, 56–81.

Falchi, M., Ortolani, F., Shi, W., Stark, C., Aloisio, G., Grizzi, S., & Dubbioso, G. (2022). 'Experimental investigation on the effect of Leading-Edge Tubercles on the Performance of Marine Propellers in fully wet condition', Ocean Engineering, 255, 111249.

Ghassemi, H., Majdfar, S., & Forouzan, H. (2016). 'Calculations of the hydrodynamic characteristics of a ducted propeller operating in oblique flow', Ship Science and Technology, 10(20), 31-40.

Gong, J., Guo, C. Y., Phan-Thien, N., & Khoo, B. C. (2020). 'Hydrodynamic loads and wake dynamics of ducted propeller in oblique flow conditions', Ships and Offshore Structures, 15(6), 645-660.

ITTC. (1999). 'ITTC–recommended procedures', International Towing Tank Conference.

Jang, H., & Mahesh, K. (2013). 'Large eddy simulation of ducted propulsors in crashback', Journal of Fluid Mechanics, 729, 151–179.

Kroll, T. B., & Mahesh, K. (2022). 'Large-eddy simulation of a ducted propeller in crashback', Flow, 2, E4.

Martio, J., Sánchez-Caja, A., & Siikonen, T. (2017). 'Open and ducted propeller virtual mass and damping coefficients by URANS method in straight and oblique flow', Ocean Engineering, 130, 92-102.

Shi, W., Atlar, M., Rosli, R., Aktas, B., & Norman, R. (2016). 'Cavitation observations and noise measurements of horizontal axis tidal turbines with biomimetic blade leading-edge designs', Ocean engineering, 121, 143-155.

Shi, W., Atlar, M. (2018) 'Hydrodynamic design of ducted propellers to enhance their efficiency in calm water conditions', Ocean Engineering, 255, 111249.

Stark, C., Shi, W., & Atlar, M. (2021). 'A numerical investigation into the influence of bio-inspired leading-edge tubercles on the hydrodynamic performance of a benchmark ducted propeller', Ocean Engineering, 237, 109593.

Stark, C., & Shi, W. (2021). 'The influence of leading-edge tubercles on the sheet cavitation development of a benchmark marine propeller', International Conference on Offshore Mechanics and Arctic Engineering, Vol. 85161. American Society of Mechanical Engineers.

Stark, C., Shi, W., & Troll, M. (2021). 'Cavitation funnel effect: Bio-inspired leading-edge tubercle application on ducted marine propeller blades', Applied Ocean Research, 116, 102864.

Stark, C., Shi, W., & Troll, M. O. R. I. T. Z. (2022). 'The Influence of Leading-Edge Tubercles on the Wake Flow Dynamics of a Marine Rudder', The 9th Conference on Computational Methods in Marine Engineering (Marine 2021).

Wang, T., Shi, H., Zhao, M., & Zhang, Q. (2023). 'Effects of a nozzle on the propeller wake in an oblique flow using modal analysis', Journal of Fluid Mechanics, 959, A14.

Yao J. (2015). 'Investigation on hydrodynamic performance of a marine propeller in oblique flow by RANS computations', International Journal of Naval Architecture and Ocean Engineering, 7(1), 56-69.